Spectral line-shape calculations for multielectron ions in hot plasmas submitted to a strong oscillating electric field

O. Peyrusse*
CELIA, Université Bordeaux I, CNRS, CEA, 351 Cours de la Libération, 33405 Talence, France
(Received 5 September 2008; published 15 January 2009)

Spectral line shapes in hot plasmas submitted to a strong oscillating electric field have been theoretically studied by applying the standard hypotheses of plasma line broadening together with a nonperturbative Floquet treatment of the external oscillating field. The formulation has been applied to the lines of nonhydrogenic emitters like He-like and Ne-like ions. It is found that the simultaneous action of a strong oscillating field and plasma particle fields can lead to dramatic changes in the spectral emission.

DOI: 10.1103/PhysRevA.79.013411 PACS number(s): 32.60.+i, 52.70.La, 32.70.Jz, 52.50.Jm

I. INTRODUCTION

The interest in studying collective plasma effects as features on spectral line shapes has a long history [1–7]. The interest in studying the effect of a strong external electric field on such a laser field is more recent and related to the advent of high-intensity lasers [8–13]. It is also important to note that the occurrence of line narrowing by using an additional monochromatic nonrandom field has been discussed in the x-ray laser context [14,15]. All of these effects correspond to the influence of an oscillating electric field (OEF) $\vec{E}=\vec{E}_L \cos \omega_{oef} t$ combined with the other fields existing in a plasma. However, it is noteworthy that collective effects can exist in an arbitrarily dense plasma where $\omega_{oef}=\omega_{pe}$ is the local plasma frequency. On the other hand, an oscillating (laser) field with $\omega_{oef}=\omega_L$ can exist only for subcritical $[N_e \leqslant N_c(\omega_L)]$ plasmas and then E_L is the local field strength. Highlighting these laser field effects gave rise to numerous studies mainly restricted to H-like ions. The increasing intensity of laser sources and their continuous application to plasma science opens the question of their influence on line emission in subcritical plasmas, and this simple question deserves consideration for the status of x-ray spectroscopy as a plasma diagnostic tool in these conditions. Of course, the simulation of a realistic time- or space-integrated line profile corresponding to some specific experiment would require a complete map of the emission as well as the map of the (more or less attenuated) laser intensity. Such a work is beyond the scope of this paper.

This paper aims at presenting a model for the computation of spectral line broadening in plasmas submitted to an arbitrary intense oscillating electric field such as the field associated with a Langmuir oscillation or the local field associated with an intense laser electric field (critical and subcritical plasmas). The method can be applied to arbitrary (nonhydrogenic) multielectron emitters, and examples of He-like and Ne-like x-ray emission are discussed. The approach follows the standard hypotheses of spectral line broadening by plasmas: namely, the impact approximation on the electrons and the quasistatic approximation for the ions [16,17]. This "standard" approach has been proven to give satisfactory results for the computation of the profile of multielectron ion emitters [18,19]. Of course, various refinements such as ion dynamics [20] or a more accurate collision operator [21–23] are possible. However, for the cases we examine in this paper, such refinements are of minor importance with regard to the effect of an additional strong oscillating electric field considered here. Another aspect of our approach is that it is based on a nonperturbative (Floquet) treatment of the OEF. The first calculations using this formalism [24] and applications [12] concerned H-like emitters. Note that the same kind of formalism has been used independently for calculating profiles of the L_α O VIII [13] and L_α F IX [6] lines. We now extend the method to nonhydrogenic emitters, and to our knowledge, this paper reports the first systematic calculations of line broadening in such atomic systems for plasmas submitted to moderate and strong OEFs. The details of our calculations are outlined below.

II. FORMALISM

The essentials of the formalism we use have been presented elsewhere [24]. We outline here the main equations, and we discuss the specific points where the nonhydrogenic character of the atomic systems under consideration is introduced. The starting point is the profile of the line radiation polarized along the vector $\vec{e}_q$ $(q=0,\pm 1)$ with $\vec{e}_0=\vec{e}_z$, $\vec{e}_{\pm 1}=\mp(\vec{e}_x \pm i\vec{e}_y)/\sqrt{2}$,

$$f_q(\omega)=\lim_{\tau->\infty}\frac{1}{2\pi\tau}\int_0^\tau dt\int_0^\tau dt' e^{i\omega(t'-t)}\phi_q(t,t'), \qquad (1)$$

where

$$\phi_q(t,t')=(-1)^q\sum_{i,f}\rho_i\{\langle\psi_i(t')|d^{(1)}_{-q}|\psi_f(t')\rangle\langle\psi_f(t)|d^{(1)}_q|\psi_i(t)\rangle\}_{ave}. \qquad (2)$$

ρ_i is the probability of a given initial state, and $\{\cdots\}_{ave}$ denotes the statistical average over the microfield distribution function and over all the possible trajectories of the perturbing electrons. $d^{(1)}_q$ are the tensorial components of the dipole operator (defined like the components of $\vec{e}_q$). Throughout this work, the ρ_i we use are simple Boltzmann factors, which

*peyrusse@celia.u-bordeaux1.fr

means that local thermal equibrium (LTE) is supposed to prevail between the initial states considered. In Eq. (2), the wave functions $|\psi\rangle$ are solutions of the Schrödinger equation $i\hbar\frac{d|\psi\rangle}{dt}=H|\psi\rangle$ with (following the standard assumptions of line broadening in plasmas) $H=H_0-\vec{d}\cdot\vec{F}-\vec{d}\cdot\vec{E}_L\cos\omega_{oef}t+V_{el}(t)$. H_0 is the free-atom Hamiltonian, $-\vec{d}\cdot\vec{F}$ is the interaction with the quasistatic ion microfield, $-\vec{d}\cdot\vec{E}_L\cos\omega_{oef}t$ is the interaction with the oscillating electric field, and $V_{el}(t)$ is the interaction with the free electrons in the plasma. The Schrödinger equation is solved in two steps. We first obtain the time-dependent function φ, which is the solution of

$$i\hbar\frac{d|\varphi\rangle}{dt}=[H_0-\vec{d}\cdot\vec{F}-\vec{d}\cdot\vec{E}_L\cos\omega_{oef}t]|\varphi\rangle, \tag{3}$$

by using the Shirley-Floquet method [25,26]. This is performed by using the eigenfunctions of H_0. Formally, Eq. (3) is equivalent to the use of the time evolution operator $S(t)=\exp[-i(H_0-\vec{d}\cdot\vec{F})t/\hbar-i\frac{\vec{d}\cdot\vec{E}_L}{\hbar\omega_{oef}}\cos\omega_{oef}t]$. In the same vein, adding the contribution of $V_{el}(t)$ is equivalent to the use of the whole evolution operator $T(t,0)=S(t)U(t,0)$. One easily sees that operator U obeys the equation $i\hbar\frac{dU}{dt}=\hat{V}_{el}U$, where $\hat{V}_{el}=S^{\dagger}V_{el}S$ is the "dressed" electron pertubation. In the present paper, and this our second step, we treat the electron perturbation $V_{el}(t)$ in the impact approximation. Although $V_{el}(t)$ should be dressed (as seen above), such a dressing normally would decrease the electron widths (Refs. [14,15]). Our findings are that electron broadening is rather small anyway compared to the other effects discussed. The validity criterion for the impact approximation is that the impact width be less than the plasma frequency which easily satisfied over a large range of plasma conditions. We note that even when this criterion is not satisfied, the impact width represents the maximum possible width and should introduce little error if electron broadening is dominated by other sources of broadening.

Another possibly limiting aspect of the formalism is related to the thermal average of operator U over a large number of individual impacts. This point is discussed below after a presentation of the method used to solve Eq. (3).

A. Outline of the Shirley-Floquet approach

This approach [25,26] is particularly appropriate for the solution of a time-dependent Schrödinger equation such as Eq. (3). It reduces the time-dependent problem to a time-independent Floquet matrix eigenvalue problem.

Following the Floquet theorem, we write the solution of Eq. (3) as

$$\varphi_{\epsilon}(\vec{r},t)=e^{-i\epsilon t/\hbar}\sum_{n,a}e^{in\omega_{oef}t}C_{\epsilon}^{(n)(a)}a(\vec{r}), \tag{4}$$

where $a(\vec{r})=\langle\vec{r}|a\rangle$, $\{|a\rangle\}$ being the complete set of eigenvectors of H_0. The coefficients $C_{\epsilon}^{(n)(a)}$ and quasienergies ϵ are obtained by diagonalizing the Floquet Hamiltonian whose matrix elements are

$$\langle b,m|H_F|a,n\rangle=h_{ba}^{(n-m)}+n\hbar\omega_{oef}\delta_{ab}\delta_{nm}, \tag{5}$$

with $h_{ba}^{(q)}=\frac{1}{\tau}\int_0^{\tau}dt\,e^{-iq\omega_{oef}t}\langle b|H_0-\vec{d}\cdot\vec{F}-\vec{d}\cdot\vec{E}\cos\omega_{oef}t|a\rangle$ and $\tau=2\pi\omega_{oef}$. Note that the Floquet states $|a,n\rangle$ are the strong-field limit of the traditional radiation-dressed atomic states. Ordering Floquet states in such a way that we run over the atomic states a before each change in n, the Floquet Hamiltonian H_F takes the block-structure form

$$\begin{array}{c} \\ n=-2 \\ n=-1 \\ n=0 \\ n=1 \\ n=2 \end{array}\begin{array}{c} \begin{array}{ccccc} n=-2 & n=-1 & n=0 & n=1 & n=2 \end{array} \\ \begin{pmatrix} \mathbf{A}-2\omega_{oef}\mathbf{I} & \mathbf{B}/2 & & & \\ \mathbf{B}/2 & \mathbf{A}-\omega_{oef}\mathbf{I} & \mathbf{B}/2 & & \\ & \mathbf{B}/2 & \mathbf{A} & \mathbf{B}/2 & \\ & & \mathbf{B}/2 & \mathbf{A}+\omega_{oef}\mathbf{I} & \mathbf{B}/2 \\ & & & \mathbf{B}/2 & \mathbf{A}+2\omega_{oef}\mathbf{I} \end{pmatrix} \end{array},$$

where $\mathbf{A}$ and $\mathbf{B}$ are, respectively, the matrices of the operators $H_0-\vec{d}\cdot\vec{F}$ and $-\vec{d}\cdot\vec{E}\cos\omega_{oef}t$, on the basis of eigenfunctions of H_0. Last, $\mathbf{I}$ is the identity matrix.

B. Profile components

We consider here the following geometry for the interaction of one ion with the oscillating field $\vec{E}$ and the microfield $\vec{F}$ (Fig. 1). Taking $\mu=\cos\theta$ where θ is the angle between $\vec{E}$ and $\vec{F}$, one has $F_{\parallel}=F\mu$ and $F_{\perp}=F\sqrt{1-\mu^2}$. Let us first consider fixed values for μ and for the amplitudes E and F. We will see below how the average over μ and F is performed. Such an average is necessary because not all of the radiating ions experience a microfield having a constant direction in space or a single field strength F. For simplicity, we just consider here the case of transitions connecting a set of upper states $\{|a\rangle\}$ and one lower state $|f\rangle$. Inserting in Eq. (2) the solution (4) (on which impacts act through the evolution operator U) leads to (after taking $s=t'-t$ and performing the integral over t)

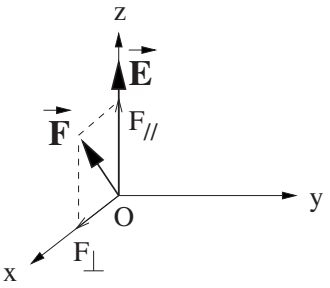

FIG. 1. Geometry for the interaction of one ion with the oscillating field **E** and plasma ion microfield **F**.

$$f_q(\omega,F,\mu,E,\omega_{oef}) = \frac{1}{2\pi}\int_{-\infty}^{+\infty} e^{i\omega s}\phi_q(s,F,\mu,E,\omega_{oef})ds, \tag{6}$$

with

$$\phi_q(s,F,\mu,E,\omega_{oef}) = (-1)^q \sum_i e^{-i\epsilon_i s/\hbar} \sum_{n,a}\sum_{a'} \rho_a e^{in\omega_{oef}s} C^{(n)(a)}_{\epsilon_i} \times C^{*(n)(a')}_{\epsilon_i} \langle a'|d^{(1)}_{-q}|f\rangle\langle f| \times \{U^\dagger(s,0)d^{(1)}_q U(s,0)\}_{ave}|a\rangle. \tag{7}$$

The sum over i runs over all the quasienergy states, and the average $\{\cdots\}$ reduces to the average over the bath of electron perturbers. Neglecting the collision-induced transitions of the type $|a\rangle - |f\rangle$ leads one to estimate matrix elements of $\{U\}$. Under the impact approximation where each impact (of duration Δt) is distinct from the others, it is possible to find a duration Δs containing many impacts so that the average over Δs takes the form

$$\{U(s,0)\} = e^{-\phi_{el}s}, \tag{8}$$

where ϕ_{el} is the electron broadening operator. In this impact approximation, such averages are made over times Δs long compared to a collision duration, but short compared to the inverse electron half-width [roughly the inverse of the matrix elements $(\phi_{el})_{aa}$]. In our context, an additional requirement arises that these averages must be taken over times long compared to the period τ_{oef} of the oscillating field, which is only possible if $\tau_{oef} \ll (\phi_{el})^{-1}_{aa}$ [or $(\phi_{el})_{aa} \ll \omega_{oef}$]. If this is not the case, averages are ill defined because the average over a time scale Δs is not always the same and depends on the exact starting time because the oscillating field is different for each Δs. In contrast, if $(\phi_{el})^{-1}_{aa} \gg \tau_{oef}$, then one can split the $(\phi_{el})^{-1}_{aa}$ time scale into smaller ones that are still large integral multiples of τ_{oef}. Note that in the case of Langmuir oscillations, this criterion also automatically satisfies the impact approximation validity criterion.

Checking the necessary inequality $\tau_{oef} \ll (\phi_{el})^{-1}_{aa}$ needs an evaluation of the electron broadening. For the examples discussed below (Sec. III), typical values for $\hbar(\phi_{el})_{aa}$ and $\hbar\omega_{oef}$ will be given. They satisfy this inequality.

Finally, we get for the profile component f_q

$$f_q(\omega,F,\mu,E,\omega_{oef}) = \frac{(-1)^q}{\pi}\sum_i \sum_{n,a}\sum_{a'} \rho_a C^{(n)(a)}_{\epsilon_i} C^{*(n)(a')}_{\epsilon_i} \times \langle a'|d^{(1)}_{-q}|f\rangle \times \langle f|d^{(1)}_q|a\rangle \frac{(\phi_{el})_{aa}}{(\phi_{el})^2_{aa} + (\omega - \omega_{if} + n\omega_{oef})^2}. \tag{9}$$

Note that this expression neglects the off-diagonal terms of the impact broadening operator. This approximation is valid when electron broadening is much smaller than the average Stark shift [19,33] (ionic microfield and/or oscillating field), which is precisely the situation considered here. Taking into account the Doppler broadening (and neglecting any correlation between the ion thermal motion and the fields) leads to replacing the Lorentzian functions with Voigt functions in Eq. (9).

Having obtained the three parts of the profile (f_0, f_1, and f_{-1}), one obtains the profile observed in the longitudinal direction $\phi_\parallel = \frac{1}{2}(f_{-1}+f_1)$ as well as the profile in the transverse direction $\phi_\perp = \frac{1}{4}(f_{-1}+f_1)+\frac{1}{2}f_0$ [24].

This expression generalizes easily to the case of transitions connecting a set of upper states and a set of lower states [24].

Last, for the electronic collision operator (which represents the effect of the electronic microfield component on the radiator), we use a well-known semiclassical expression [27] which is averaged over a Maxwellian distribution for the electron perturbers. Although the actual distribution should differ from a pure Maxwellian due to effect of the oscillating field (see, for instance, [28]), we disregard this difference, because as mentioned above, electron broadening is small in all the cases of hot dense plasmas considered in this paper (Sec. III).

C. Matrix elements of the dipole operator

Matrix elements of the dipole operator are involved in the expression of the line profile itself [see Eq. (9)], as well as in the Floquet matrix, where

$$A_{aa'} = \langle a|H_0|a'\rangle + \frac{1}{\sqrt{2}}(d^{(1)}_1)_{aa'}F_\perp - \frac{1}{\sqrt{2}}(d^{(1)}_0)_{aa'}F_\parallel - \frac{1}{\sqrt{2}}(d^{(1)}_{-1})_{aa'}F_\perp, \tag{10}$$

$$B_{aa'} = -\frac{1}{\sqrt{2}}(d^{(1)}_0)_{aa'}E. \tag{11}$$

In units of $-ea_0$, the qth component of the dipole operator takes the form $d^{(1)}_q = \frac{4\pi}{3}\Sigma_{i=1}^N r_i Y_{1q}(\hat{r}_i)$, where N is the number of electrons in the atomic system under consideration. In [24], we limited ourself to hydrogenic systems ($N=1$) for which exact analytical values of these matrix elements can be found. For arbitrary nonhydrogenic emitters, the states $|a\rangle$ correspond to a set of *coupled* states $|\gamma JM\rangle$ as defined in the theory of atomic structure [29]. A further well-known expres-

sion follows from the application of the Wigner-Eckart theorem:

$$\langle \gamma JM|d_q^{(1)}|\gamma' J' M'\rangle = (-1)^{J-M}\begin{pmatrix} J & 1 & J' \\ -M & q & M' \end{pmatrix}\langle \gamma J\|d^{(1)}\|\gamma' J'\rangle,$$

where the reduced matrix element $\langle \gamma J\|d^{(1)}\|\gamma' J'\rangle$ can be evaluated from an atomic structure code that finds the coupled states diagonalizing H_0. Those states are usually built using a combination of Slater determinants made of one-electron atomic orbitals. Each of these orbitals is the solution of a one-electron Schrödinger equation with an averaged (self-consistent or not) radial potential. Various approaches have been developed to build this potential. Here, we have used an approximation [30] to the optimized effective potential approach [31]. The subsequent construction of the atomic states from Slater determinants is purely numerical (without any Racah algebra) and based on direct diagonalization [32].

D. Integral over the microfield distribution function

Choosing Oz as the axis of $\vec{E}_L$ means that the microfield $\vec{F}$ is randomly distributed with respect to that axis. Taking the field strength F and $\mu=\cos\theta$ as integration variables, we write for the profile of component q

$$F_q(\omega,E,\omega_{oef}) = \frac{1}{2}\int_0^\infty W(F)dF\int_{-1}^{+1} d\mu\, f_q(\omega,F,\mu,E,\omega_{oef}), \tag{12}$$

where $F_\parallel=F\mu$ and $F_\perp=F\sqrt{1-\mu^2}$ in expressions (10) and (11) and, then, in the Floquet matrix. In Eq. (12), $W(F)$ is the microfield distribution for which we used a fit of numerous Monte Carlo simulations [33,34]. This fit does not depend on the oscillating electric field while the actual $W(F)$ should because of the electronic screening of the ions which can be affected by this field. We have disregarded this possible difference because our prime objective is to describe features in the profiles which are mainly due to the interaction term $-\vec{d}\cdot\vec{E}_L\cos\omega_{oef}t$ in the Hamiltonian.

III. RESULTS

As mentioned above, the present formalism has already been used for H-like emitters [13,24]. In view of exhibiting significant examples of nonhydrogenic line profiles that could be strongly affected by an oscillating electric field, the present version of our corresponding computer code has been applied to He-like and Ne-like emitters. As a first application, we calculated the Al He$_\beta$ line profile for a density $N_e=3\times10^{22}$ cm^{-3}, a temperature $T_e=300$ eV, and an oscillating field of amplitude $E=2F_0$, where $F_0=Z^*e/r_0^2$ is the Holtsmark normal field (r_0 is the ion-sphere radius). Here the frequency ω_{oef} is the local plasma frequency $\hbar\omega=6.43$ eV. We found that the electron full width at half maximum (FWHM) was of the order a few tenths of eV. Results for $\phi_\parallel$ and $\phi_\perp$ are plotted in Fig. 2. The expected two satellites (indicated by the arrows) at $\pm\hbar\omega$ are clearly visible on both sides of the line. Such satellites could be the local signature of a nonthermal field arising from the excitation of Langmuir waves in a dense plasma.

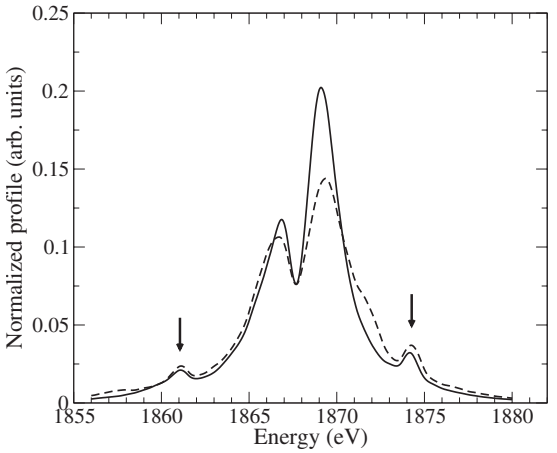

FIG. 2. Al He$_\beta$, $N_e=3\times10^{22}$ cm^{-3}. $\hbar\omega=6.43$ eV. $E=2F_0$. Solid line: $\phi_\parallel$. Dashed line: $\phi_\perp$.

We have also used the present model to calculate the Al K-shell $n=2$-1 He$_\beta$, He$_\gamma$, and He$_\delta$ lines for a temperature $T_e=300$ eV, density $N_e=N_c$ $(=1.1\times10^{21}/\lambda_L^2)$ with $\lambda_L=0.79$ μm—i.e., $\hbar\omega_L=1.569$ eV (Ti-sapphire laser)—and various laser intensities. The electron FWHM has been found to lie between a few hundredths of eV (He$_\beta$) and a few tenths of eV (He$_\gamma$,He$_\delta$). For comparison, the Doppler width is of the order of a few tenths of eV in these conditions. For each value of the intensity, we carefully checked the convergence with the number of Floquet blocks (equal to $2n_F+1$, where $n_F=0,1,2,\ldots$ is the number of Floquet modes; see Sec. II A) needed to obtain a correct result. Note that for important field amplitudes corresponding to high laser intensities $I_L>10^{17}$ W/cm^2, this number can be as large as 21 and thus leads to large Floquet matrices to diagonalize when the number of atomic states considered is already large. Such a convergence is illustrated in Fig. 3 where we plotted the He$_\beta$ line ($\phi_\parallel$) in a plasma with $I_L=10^{15}$ W/cm^2, for four calculations

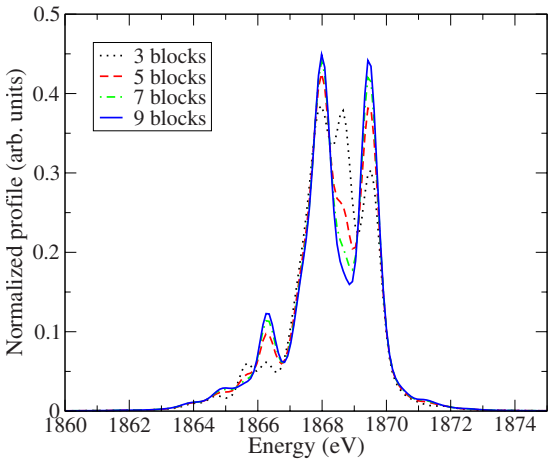

FIG. 3. (Color online) Calculation of the Al He$_\beta$ line profile ($\phi_\parallel$) at 10^{15} W/cm^2, $N_e=N_c$, $T_e=300$ eV, and $\lambda_L=0.79$ μm, as a function of the number of Floquet blocks.

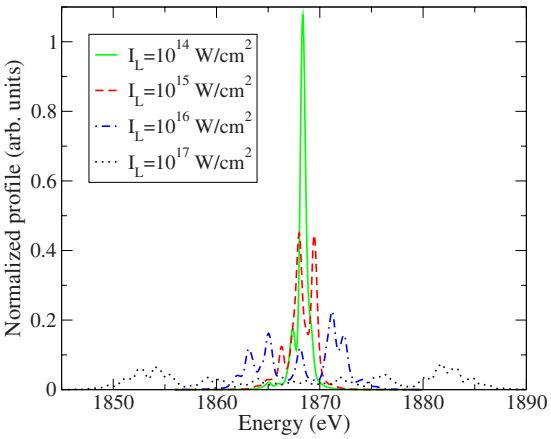

FIG. 4. (Color online) Various Al He$_\beta$ profiles as a function of the laser intensity. At 10^{14} W/cm^2, the profile is identical to a no-laser-field calculation.

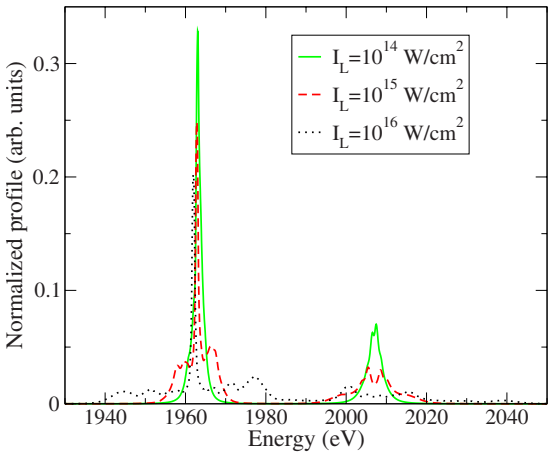

FIG. 5. (Color online) Simultaneous calculations of the n=4-1 and n=5-1 (He$_\gamma$, He$_\delta$) profiles ($\phi_\parallel$) as a function of the laser intensity. At 10^{14} W/cm^2, the profile is identical to a no-laser-field calculation.

with 3, 5, 7, and 9 Floquet blocks, respectively.

For the above plasma conditions (and with $\hbar\omega_L$ =1.569 eV) the effect of an increasing laser field on the parallel component ($\phi_\parallel$) of the He$_\beta$ line is displayed in Fig. 4. We note here the very strong effect of an intense local laser field that results in a large spread of the various components of the line including the field-induced satellites. More precisely, according to the field strength, we observe different distributions of intensity among the components of the line. The profiles being normalized, the line disappears almost completely for $I_L > 10^{17}$ W/cm^2 while for I_L less than about 10^{14} W/cm^2, the profile is identical to a no-laser-field calculation. It is noteworthy that for laser intensities of about 10^{15} W/cm^2, the He$_\beta$ line shows a strong dip for densities for which calculations without oscillating electric field exhibit no dip. A hole in the He$_\beta$ line is expected at much higher densities (see Fig. 2, for instance) although, in that case, ion dynamical effects have been shown to fill that dip.

It may be interesting to see the effect of an oscillating electric field on a slightly more complicated atomic structure where an important mixing is expected. For that purpose, we looked at the profiles of the He$_\gamma$ and He$_\delta$ lines by calculating simultaneous K-shell emission from the sets of all the $1sn\ell$ (n=4,5) states. The results are shown in Fig. 5. Such a mixing is obvious for $I_L > 10^{16}$ W/cm^2. At $I_L > 10^{15}$ W/cm^2 an apparent broadening of the lines is also noticeable as well as an apparent shift of He$_\gamma$. Note that such a broadening could lead to an erroneous density diagnostic of the plasma if the emitting zone (with such a possibly present field) is analyzed discarding the field effect.

Ne-like L-shell n=3-2 emission presents specific characteristics which have been used for the diagnostic of a mid-Z laser-produced plasma. The effect of a strong oscillating field on these specific emission features (which are known for having much less sensitivity to Stark ion broadening than K-shell emission features) is thus interesting. Considering the whole set of upper states belonging to configurations $1s^22s^22p^53s$, $1s^22s^22p^53p$, $1s^22s^22p^53d$, $1s^22s2p^63s$, $1s^22s2p^63p$, and $1s^22s2p^63d$, we performed calculations of the Ge n=3-2 emission for a few values of the laser intensity with λ_L=0.79 μm. In these calculations, N_e=N_c and T_e =400 eV. Results are displayed in Fig. 6. For the lower value of the laser intensity, Fig. 6(a), one recognizes the well-known lines $3p$-$2s$ (A, B), $3d$-$2p$ (C, D, E), and $3s$-$2p$ (F, G) [35]. As expected, one sees less sensitivity to the laser field than the He-like Al emission. At $I_L \geqslant 10^{18}$ W/cm^2, however, field mixing becomes important. It is noteworthy here that in actual emission spectra, the Ne-like emission is superimposed on the emission of adjacent ions (Na-like satellites, F-like, O-like, etc.), although Ne-like lines remain preminent. For large values of the laser field, these calculations indicate an important field-induced broadband emission.

As possible candidates for observing satellite lines induced by a laser field, the L-shell n=3-2 transitions in a He-like ion such as Mg^{10+} (Mg XI spectrum) have been proposed [8]. The level structure here is very close to the original scheme proposed by Baranger and Mozer (BM) [1] for observing an oscillating-field-induced satellite structure—i.e., a forbidden line $3p$-$2p$ very close to the allowed one $3d$-$2p$. We have calculated the whole Mg XI n=3-2 emission in presence of an electric field oscillating at

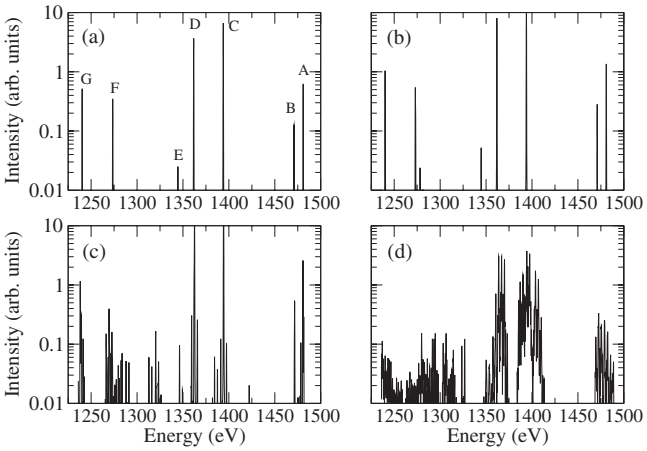

FIG. 6. Ne-like emission (of the type ∥) of Ge (T_e=400 eV, N_e=N_c, λ_L=0.79 μm, Z^*=22). (a) 10^{15} W/cm^2, (b) 10^{16} W/cm^2, (c) 10^{17} W/cm^2, and (d) 10^{18} W/cm^2.

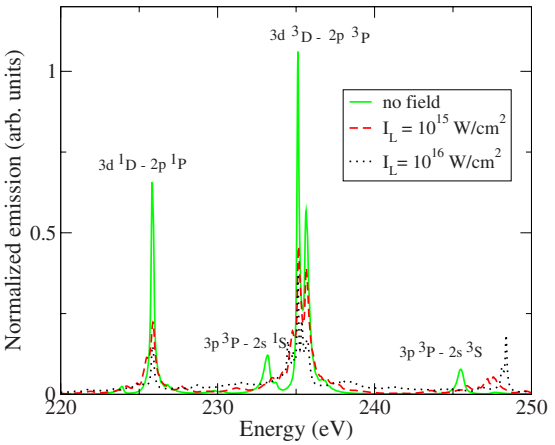

FIG. 7. (Color online) Mg XI (He-like) ($1s3d$, $1s3p$, $1s3s$) to ($1s2s$, $1s2p$) transitions (of the type $\|$) with $\hbar\omega_L$=3.51 eV for a frequency-tripled 1.06-μm laser. N_e=0.5N_c, T_e=200 eV.

$\hbar\omega_L$=3.51 eV—i.e., for a frequency-tripled 1.06-μm laser. In these calculations, N_e=0.5N_c and T_e=200 eV. We did not observe a clear BM-like behavior in the spectrum. The mixing introduced by the field is so important that no clear evidence of satellites has been found. Results of calculations for a few values of the laser intensity are given in Fig. 7.

IV. CONCLUSIONS

We have presented a line-shape model which takes into account the influence of an arbitrary intense oscillating electric field in addition to the effect of other fields (ionic and electronic) existing in a plasma. Such a model can be applied to nonhydrogenic emitters. For relatively low electric fields—i.e., of the order of magnitude of the ion microfield—calculations give additional evidence that satellites to spectral lines are of potential use in measuring fundamental parameters in plasmas. We have also shown that a complicated atomic structure—i.e., a complicated set of radiatively coupled states—when submitted to a strong oscillating electric field, gives rise to very complicated spectral features. For some cases, lines disappear, while groups of lines can merge into broad structures that cannot be clearly identified anymore. Such calculations suggest that care must be put into the analysis of the radiation emitted by subcritical or nearly critical zones of laser-produced plasmas, more especially as they are by far the most emitting.

Further improvements will concern the use of a more accurate collision operator or the use of non-LTE populations.

ACKNOWLEDGMENT

The author gratefully acknowledges valuable comments of the referees.

[1] Michel Baranger and Bernard Mozer, Phys. Rev. **123**, 25 (1961).
[2] Tsu-Jye A. Nee and H. R. Griem, Phys. Rev. A **14**, 1853 (1976).
[3] R. W. Lee, J. Phys. B **12**, 1165 (1979).
[4] C. Deutsch and G. Bekefi, Phys. Rev. A **14**, 854 (1976).
[5] E. A. Oks, St. Böddeker, and H.-J. Kunze, Phys. Rev. A **44**, 8338 (1991).
[6] V. P. Gavrilenko, V. S. Belyanev, A. S. Kurilov, A. P. Matafonov, V. I. Vinogradov, V. S. Lisitsa, A. Ya. Faenov, T. A. Pikuz, I. Yu. Skobelev, A. I. Magunov, and S. A. Pikuz, Jr., J. Phys. A **39**, 4353 (2006).
[7] N. C. Woolsey, J. Howe, D. M. Chambers, C. Courtois, E. Förster, C. D. Gregory, I. M. Hall, O. Renner, and I. Uschmann, High Energy Density Phys. **3**, 292 (2007).
[8] R. C. Elton, H. R. Griem, B. L. Welch, A. L. Osterheld, R. C. Mancini, J. Knauer, G. Pien, R. G. Watt, J. A. Cobble, P. A. Jaanimagi, D. K. Bradley, J. A. Delettrez, and R. Epstein, J. Quant. Spectrosc. Radiat. Transf. **58**, 559 (1997).
[9] I. Y. Skobelev, A. Y. Faenov, A. I. Magunov, A. Osterheld, B. Young, J. Dunn, and R. E. Stewart, Phys. Scr. **T73**, 104 (1997).
[10] S. A. Pikuz, A. Maksimchuk, D. Umstadter, M. Nantel, I. Y. Skobelev, A. Y. Faenov, and A. Osterheld, JETP Lett. **66**, 480 (1997).
[11] A. Maksimchuk, M. Nantel, G. Ma, S. Gu, C. Y. Cote, D. Umstadter, S. A. Pikuz, I. Y. Skobelev, and A. Y. Faenov, J. Quant. Spectrosc. Radiat. Transf. **65**, 367 (2000).
[12] O. Renner, O. Peyrusse, P. Sondhauss, and E. Forster, J. Phys. B **33**, L151 (2000).
[13] V. P. Gavrilenko, A. Ya. Faenov, A. I. Magunov, T. A. Pikuz, I. Yu. Skobelev, K. Y. Kim, and H. M. Milchberg, Phys. Rev. A **73**, 013203 (2006).
[14] E. Oks, J. Phys. B **33**, L801 (2000).
[15] S. Alexiou, J. Quant. Spectrosc. Radiat. Transf. **71**, 139 (2001).
[16] Michel Baranger, Phys. Rev. **111**, 481 (1958); **111**, 494 (1958); **112**, 855 (1958).
[17] A. C. Kolb and H. Griem, Phys. Rev. **111**, 514 (1958).
[18] L. A. Woltz and C. F. Hooper, Jr., Phys. Rev. A **38**, 4766 (1988).
[19] A. Calisti, F. Khelfaoui, R. Stamm, B. Talin, and R. W. Lee, Phys. Rev. A **42**, 5433 (1990).
[20] B. Talin, A. Calisti, L. Godbert, R. Stamm, R. W. Lee, and L. Klein, Phys. Rev. A **51**, 1918 (1995).
[21] S. Alexiou, Phys. Rev. A **49**, 106 (1994).
[22] S. Alexiou and Y. Maron, J. Quant. Spectrosc. Radiat. Transf. **53**, 109 (1995).
[23] A. Könies and S. Günter, Phys. Rev. E **52**, 6658 (1995).
[24] O. Peyrusse, Phys. Scr. **56**, 371 (1997).
[25] J. H. Shirley, Phys. Rev. **138**, B979 (1965).
[26] Shih-I Chu, Adv. At. Mol. Phys. **21**, 197 (1985).
[27] H. R. Griem, M. Blaha, and P. C. Kepple, Phys. Rev. A **19**, 2421 (1979).
[28] B. N. Chichkov, S. A. Shumsky, and S. A. Uryupin, Phys. Rev. A **45**, 7475 (1992).
[29] R. D. Cowan, *The Theory of Atomic Structure and Spectra* (University of California Press, Berkeley, CA, 1981).

[30] J. B. Krieger, Yan Li, and G. J. Iafrate, Phys. Rev. A **46**, 5453 (1992).
[31] J. D. Talman and W. F. Shadwick, Phys. Rev. A **14**, 36 (1976).
[32] E. U. Condon and G. H. Shortley, *The Theory of Atomic Spectra* (Cambridge University Press, London, 1951).
[33] D. Gilles and O. Peyrusse, J. Quant. Spectrosc. Radiat. Transf. **53**, 647 (1995).
[34] A. Y. Potekhin, G. Chabrier, and D. Gilles, Phys. Rev. E **65**, 036412 (2002).
[35] P. G. Burkhalter, D. J. Nagel, and R. D. Cowan, Phys. Rev. A **11**, 782 (1975).